0026-895X/04/6603-561–571$20.00
MOLECULAR PHARMACOLOGY
Copyright © 2004 The American Society for Pharmacology and Experimental Therapeutics
Mol Pharmacol 66:561–571, 2004

Vol. 66, No. 3
3221/1170073
Printed in U.S.A.

YC-1-Induced Cyclooxygenase-2 Expression Is Mediated by cGMP-Dependent Activations of Ras, Phosphoinositide-3-OH-kinase, Akt, and Nuclear Factor-κB in Human Pulmonary Epithelial Cells

Ming-Shyan Chang, Wen-Sen Lee, Bing-Chang Chen, Joen-Rong Sheu, and Chien-Huang Lin

Graduate Institute of Medical Sciences (M.-S.C., W.-S.L., J.-R.S.), School of Respiratory Therapy (B.-C.C., C.-H.L.), and Graduate Institute of Biomedical Technology (C.-H.L.), College of Medicine, Taipei Medical University, Taipei, Taiwan

Received January 16, 2004; accepted June 2, 2004

This article is available online at http://molpharm.aspetjournals.org

ABSTRACT

We demonstrated previously that 3-(5′-hydroxymethyl-2′-furyl)-1-benzylindazole (YC-1), an activator of soluble guanylate cyclase (sGC), induces cyclooxygenase-2 (COX-2) expression via cGMP- and p44/42 mitogen-activated protein kinase-dependent pathways in human pulmonary epithelial A549 cells. In this study, we explore the role of Ras, phosphoinositide-3-OH-kinase (PI3K), Akt, and transcription factor nuclear factor-κB (NF-κB) in YC-1–induced COX-2 expression in A549 cells. A Ras inhibitor (manumycin A), a PI3K inhibitor (wortmannin), an Akt inhibitor (1L-6-Hydroxymethyl-chiro-inositol2-[(*R*)-2-*O*-methyl-3-*O*-octadecylcarbonate]), and an NF-κB inhibitor [pyrrolidine dithiocarbamate (PDTC)] all reduced YC-1–induced COX-2 expression. The YC-1–induced increase in COX activity was also blocked by manumycin A, wortmannin, PDTC, and the dominant-negative mutants for Ras (RasN17), Akt (Akt DN), and IκBα (IκBαM). The YC-1–induced increase in Ras activity was inhibited by an sGC inhibitor [1*H*-(1,2,4)oxadiazolo[4,3-*a*]quinozalin-1-one (ODQ)], a protein kinase G (PKG) inhibitor [1-oxo-9.12-epoxy-1*H*-diindolo[1,2,3-*fg*:3′,2′,1′-kl]pyrrolo[3,4-l][1,6]benzodiazocine-10-carboxylic acid methyl ester (KT-5823)], and manumycin A. YC-1–induced Akt activation was also inhibited by ODQ, KT-5823, manumycin A, and wortmannin. YC-1 caused the formation of an NF-κB–specific DNA-protein complex and an increase in κB-luciferase activity. YC-1–induced κB-luciferase activity was inhibited by ODQ, KT-5823, manumycin A, wortmannin, an Akt inhibitor, PDTC, RasN17, Akt DN, and IκBαM. Likewise, YC-1–induced IKKα/β activation was inhibited by ODQ, KT-5823, manumycin A, wortmannin, and an Akt inhibitor. Furthermore, YC-1–induced COX-2 promoter activity was inhibited by manumycin A, RasN17, Akt DN, PDTC, and IκBαM. Taken together, these results indicate that YC-1 might activate the sGC/cGMP/PKG pathway to induce Ras and PI3K/Akt activation, which in turn initiates IKKα/β and NF-κB activation and finally induces COX-2 expression in A549 cells.

Prostaglandins (PGs), lipid mediators, play important roles in many biological processes, including cell division, blood pressure regulation, immune responses, ovulation, bone development, wound healing, and water balance. Altered prostanoid production is associated with a variety of illnesses, including long- and short-term inflammation, cardiovascular disease, colon cancer, and allergic diseases (DeWitt, 1991; Smith and Marnett, 1991). Cyclooxygenase (COX) catalyzes the conversion of arachidonic acid to prostaglandin H_2 (PGH_2), which is then further metabolized to various PGs, prostacyclin, and thromboxane A_2 (Vane et al., 1998). Two COX isoforms, COX-1 and COX-2, have been identified in humans (Mitchell et al., 1995). COX-1 is generally thought to produce prostaglandins, which serve to maintain cellular homeostasis, and is known to be expressed constitutively in many cell types, including endothelial cells, platelets, and gastric mucosa (Vane 1994), whereas COX-2 is inducibly expressed in most mammalian cells. COX-2 expression occurs rapidly by cytokines, growth factors, or bacterial endotoxin stimulation (Vane et al., 1998; Lin et al., 2001). COX-2 plays a major role in inflammatory processes, and its

This work was supported by a research grant (NSC91-2314-B-038-010) from the National Science Council of Taiwan.

ABBREVIATIONS: COX, cyclooxygenase; PG, prostaglandin; YC-1, 3-(5′-hydroxymethyl-2′-furyl)-1-benzylindazole; sGC, soluble guanylate cyclase; PKG, protein kinase G; PKC, protein kinase C; MAPK, mitogen-activated protein kinase; PI3K, phosphoinositide-3-OH-kinase; NF-κB, nuclear factor-κB; IL, interleukin; ODQ, 1*H*-(1,2,4)oxadiazolo[4,3-*a*]quinozalin-1-one; DMEM, Dulbecco's modified Eagle's medium; FCS, fetal calf serum; IKK, IκB kinase; IκB, inhibitor of NF-κB; DN, dominant negative; PAGE, polyacrylamide gel electrophoresis; PBS, phosphate-buffered saline; PMSF, phenylmethylsulfonyl fluoride; DTT, dithiothreitol; PDTC, pyrrolidine dithiocarbamate.

expression has been linked with several diseases associated with inflammation and colon cancer (Williams et al., 1999).

3-(5′-Hydroxymethyl-2′-furyl)-1-benzylindazole (YC-1) has been identified as an activator of soluble guanylate cyclase (sGC), and was shown to increase the intracellular cGMP concentration in platelets (Ko et al., 1994). The cGMP-increasing effect of YC-1 has been reported to mediate tracheal relaxation (Hwang et al., 1999) and vascular protection (Tulis et al., 2002). It was further demonstrated that YC-1 not only stimulated sGC but also inhibited cGMP-hydrolyzing phosphodiesterase in human platelets (Friebe et al., 1998). Our previous study demonstrated that YC-1 activates protein kinase G (PKG) through an upstream sGC/cGMP pathway to induce protein kinase C (PKC)-α and p44/42 mitogen-activated protein kinase (MAPK) activation, which in turn induces COX-2 expression in human pulmonary epithelial cells (Chang et al., 2002). However, the molecular mechanism underlying YC-1–induced cyclooxygenase-2 expression remains to be determined.

Ras has been linked to numerous effector pathways that lead to the induction of diverse physiological and pathological responses. These pathways regulate cell proliferation, cytoskeleton change, or the release of proinflammatory mediators (Campbell et al., 1998; Reddy et al., 2000). It has been demonstrated recently that up-regulation of COX-2 is a downstream effector of Ras-mediated transformation in mammary epithelial cells (Subbaramaiah et al., 1996). Oncogenic mutations of Ras result in activation of downstream signaling molecules, including the Raf, MAPK/extracellular signal-regulated kinase kinase, p44/42 MAPK (McCormick, 1994), and phosphoinositide-3-OH-kinase (PI3K)/Akt (Rodriguez-Viciana et al., 1997) pathways.

Akt, a serine/threonine kinase, is a direct downstream effector of PI3K (Franke et al., 1997). Akt can be modulated by multiple intracellular signaling pathways and acts as a transducer for many pathways initiated by growth factor receptor-activated PI3K. The PI3K/Akt pathway plays a critical role in Ras-mediated cellular transformation, adhesion, and survival (Osada et al., 1999). In addition, Akt can stimulate signaling pathways that up-regulate the activity of the transcription factor nuclear factor-κB (NF-κB), in the Jurkat T-cell (Kane et al., 1999). The transcription factor NF-κB has been shown to be important in inflammation, in suppression of apoptosis, and in cell proliferation (Baldwin, 1996; Tak and Firestein, 2001). In addition, NF-κB has been shown to control transcription of the *COX-2* gene (Schmedtje et al., 1997). Moreover, recent reports have demonstrated that oncogenic Ras-induced signaling activates NF-κB transcriptional activity, which is required for cellular transformation (Finco et al., 1997).

The roles of Ras, PI3K/Akt, and NF-κB in YC-1–induced COX-2 expression remain unclear. Therefore, the objective of this study was to identify the roles of Ras, PI3K/Akt, and NF-κB in YC-1–induced COX-2 expression in human pulmonary epithelial cells. The findings revealed that cGMP/PKG-dependent activation of Ras, PI3K/Akt, and NF-κB plays an important role in YC-1–mediated COX-2 expression in human pulmonary epithelial cells (A549).

Materials and Methods

Materials. YC-1, 8-bromo-cGMP, interleukin-1β (IL-1β), 1*H*-(1,2,4)oxadiazolo[4,3-*a*]quinozalin-1-one (ODQ), KT-5823, manumycin A, and wortmannin were purchased from Calbiochem-Novabiochem (San Diego, CA). The Akt inhibitor 1L-6-hydroxymethyl-chiro-inositol2-[(*R*)-2-*O*-methyl-3-*O*-octadecylcarbonate] was purchased from Alexis (Läufelfingen, Switzerland). Dulbecco's modified Eagle's medium (DMEM)/Ham's F-12, fetal calf serum (FCS), and penicillin/streptomycin were purchased from Invitrogen (Carlsbad, CA). [γ-^{32}P]ATP was purchased from Amersham Biosciences (Little Chalfont, Buckinghamshire, UK). A PGE_2 enzyme immunoassay kit was purchased from Cayman Chemical (Ann Arbor, MI). Antibody specific for COX-2 was purchased from BD Transduction Laboratories (Lexington, KY). Protein A/G beads, IκBα protein (amino acids 1~317), rabbit polyclonal antibodies specific for IκB kinase (IKK) α/β and Akt, as well as horseradish peroxidase-conjugated anti-mouse and anti-rabbit antibodies were purchased from Santa Cruz Biotechnology (Santa Cruz, CA). Antibodies specific for phospho-Akt (Ser473) and phospho-IKKα (Ser180)/IKKβ (Ser181) were purchased from New England Biolabs (Beverly, MA). An antibody specific for α-tubulin was purchased from Oncogene Science (Cambridge, UK). Anti-mouse IgG-conjugated alkaline phosphatase was purchased from Jackson ImmunoResearch Laboratories (West Grove, PA). 4-Nitro blue tetrazolium and 5-bromo-4-chloro-3-indolyl-phosphate were purchased from Roche Applied Science (Mannheim, Germany). The enhanced chemiluminescence detection agent was purchased from PerkinElmer Life and Analytical Sciences (Boston, MA). A dominant-negative Ras mutant (RasN17) and a Ras activity assay kit were purchased from Upstate Biotechnology (Lake Placid, NY). A dominant-negative IκBα mutant (IκBαM) was purchased from BD Biosciences (Palo Alto, CA). A dominant-negative Akt mutant (Akt DN) was a kind gift from Prof. C.-M. Teng (National Taiwan University, Taipei, Taiwan). pGL2-ELAM-Luc, which is under the control of one NF-κB binding site, and pBK-CMV-Lac Z were kindly provided by Prof. W.-W. Lin (National Taiwan University, Taipei, Taiwan). A human COX-2 promoter-luciferase construct, pGS459 (−459/+9), which contains 2 κB binding sites, was a kind gift from Prof. C.-C. Chen (National Taiwan University, Taipei, Taiwan). All materials for SDS-PAGE were obtained from Bio-Rad (Hercules, CA). All other chemicals were obtained from Sigma (St. Louis, MO).

Cell Culture. A549 cells, a human pulmonary epithelial carcinoma cell line with type II alveolar epithelial cell differentiation, were obtained from the American Type Culture Collection (Manassas, VA) and grown in DMEM/Ham's F-12 nutrient mixture containing 10% FCS and penicillin/streptomycin (50 U/ml) in a humidified 37°C incubator. After the cells had grown to confluence, they were disaggregated in a trypsin solution, washed in DMEM/Ham's F-12 supplemented with 10% FCS, centrifuged at 125*g* for 5 min, resuspended, and then subcultured according to standard protocols. Cells were seeded onto 10-cm dishes for the electrophoretic mobility shift assay, immunoblotting, or kinase assays or onto 12-well plates for COX-2 promoter-luciferase assays, κB-luciferase assays, or PGE_2 enzyme immunoassay.

Measurement of COX Activity and PGE_2 Release. A549 cells were cultured in 12-well culture plates. For experiments designed to measure the COX activity, cells were treated with YC-1 for 12 h, washed with phosphate-buffered saline (PBS), and then treated with fresh medium containing arachidonic acid (30 μM) for 30 min at 37°C. The media were then collected for the PGE_2 enzyme immunoassay according to the procedure described by the manufacturer. In some experiments, cells were either pretreated with specific inhibitors as indicated, or transfected with the dominant-negative mutants for Ras (RasN17), Akt (Akt DN), or IκBα (IκBαM) followed by YC-1 and incubated at 37°C for 12 h. After incubation, cells were washed and then treated with fresh medium containing arachidonic acid (30 μM) for 30 min at 37°C; the medium was then collected for the PGE_2 enzyme immunoassay. In the experiments designed to measure the PGE_2 release, the cells were treated with YC-1 (50 μM), IL-1β (0.1~1 ng/ml), or a combination of YC-1 (50 μM) and IL-1β (0.1~1 ng/ml) for 12 h. After treatment, the media were then collected for the PGE_2 enzyme immunoassay.

Protein Preparation and Western Blotting. To determine the levels of COX-2, α-tubulin, phospho-Akt (Ser473), Akt, phospho-IKKα (Ser180)/IKKβ (Ser181), and IKKα/β in A549 cells, the proteins were extracted, and Western blot analysis was performed as described previously (Chang et al., 2002). In brief, A549 cells were cultured in 10-cm dishes. After reaching confluence, cells were treated with YC-1 or 8-bromo-cGMP, or pretreated with specific inhibitors as indicated followed by YC-1, and incubated in a humidified incubator at 37°C. After incubation, cells were washed with PBS, incubated with extraction buffer (10 mM Tris, pH 7.0, 140 mM NaCl, 2 mM PMSF, 5 mM DTT, 0.5% Nonidet P-40, 0.05 mM pepstatin A, and 0.2 mM leupeptin) with gentle shaking, and then centrifuged at 12,500 rpm for 30 min. The cell extract was then boiled in sample buffer (100 mM Tris, pH 6.8; 20% glycerol, 4% SDS, and 0.2% bromphenol blue) at a ratio of 1:1. Electrophoresis was performed using 10% SDS-polyacrylamide gels (2 h, 110 V, 40 mA, 40 μg of protein per lane). Separated proteins were transferred to polyvinylidene difluoride membranes (2 h, 40 V), treated with 5% fat-free milk powder to block the nonspecific IgGs, and incubated for 2 h with specific antibodies for COX-2, α-tubulin, phospho-Akt (Ser473), Akt, phospho-IKKα (Ser180)/IKKβ (Ser181), or IKKα/β. The blot was then incubated with anti-mouse or anti-rabbit IgG linked to alkaline phosphatase or horseradish peroxidase for 2 h. Thereafter, the immunoreactivity was detected with 4-nitro blue tetrazolium/5-bromo-4-chloro-3-indolyl-phosphate as a substrate or by enhanced chemiluminescence. Quantitative data were obtained using a computing densitometer with Image-Pro plus software (Media Cybernetics, Silver Spring, MD).

Transfection and Luciferase Reporter Assays. A549 cells (2.5×10^5) were seeded into 12-well plates. For the COX-2 promoter and κB-luciferase assay, cells were transfected on the following day with the LipofectAMINE Plus reagent containing 1 μg of pGS459 (−459/+9) or 0.5 μg of pGL2-ELAM-Luc, respectively, and 1 μg of pBK-CMV-LacZ for 24 h. After incubation, the medium was aspirated and replaced with fresh DMEM/Ham's F12 containing 10% FCS. Cells were then stimulated with YC-1 for another 24 h before harvesting. To assay the effects of various inhibitors, drugs were added to the cells 30 min before YC-1 stimulation. To assay the effects of various dominant-negative mutants (RasN17, Akt DN, and IκBαM), mutants were cotransfected with pGS459 (−459/+9) and pBK-CMV-LacZ or pGL2-ELAM-Luc and pBK-CMV-LacZ for 24 h, and then treated with YC-1. Luciferase activity was determined with a luciferase assay system (Promega) and normalized based on LacZ expression. The level of induction of luciferase activity was determined as a ratio of stimulated and unstimulated cells.

Immunoprecipitation and IKKα/β Kinase Assays. A549 cells were grown in 6-cm dishes. After reaching confluence, cells were treated with YC-1 for 0~60 min, or pretreated with specific inhibitors as indicated followed by YC-1. After incubation, cells were washed twice with ice-cold phosphate-buffered saline, lysed in 1 ml of lysis buffer containing 20 mM Tris-HCl, pH 7.5, 1 mM $MgCl_2$, 125 mM NaCl, 1% Triton X-100, 1 mM PMSF, 10 μg/ml leupeptin, 10 μg/ml aprotinin, 25 mM β-glycerophosphate, 50 mM NaF, and 100 μM sodium orthovanadate, and centrifuged. The supernatant was then immunoprecipitated with a polyclonal antibody against IKKα/β in the presence of A/G-agarose beads overnight. The beads were washed three times with lysis buffer and two times with kinase buffer (20 mM HEPES, pH 7.4, 20 mM $MgCl_2$, and 2 mM DTT). The kinase reactions were performed by incubating immunoprecipitated beads with 20 μl of kinase buffer supplemented with 2.5 μg of bacterially expressed GST-IκBα (amino acids 5~55), 20 μM ATP, and 3 μCi of [γ-^{32}P]ATP at 30°C for 30 min. The reaction mixtures were analyzed by 12% SDS-PAGE followed by autoradiography.

Ras Activity Assay. Ras activity was assayed using a Ras activation assay system (Upstate Biotechnology) according to the procedure described by the manufacturer. In brief, cell lysates (0.5~1 mg) were incubated on a rocker plate at 4°C for 30 min with 10 μg of Ras-binding domain for Raf-1 bound to glutathione agarose beads. The beads were then extensively washed with Mg-containing lysis buffer (25 mM HEPES, pH 7.5; 150 mM NaCl, 10% glycerol, 5% Igepal CA-630, 1 mM EDTA, and 10 mM $MgCl_2$). Bound Ras proteins were then solubilized in 2× Laemmli sample buffer and quantitatively detected by Western blotting (15% SDS-PAGE) using a mouse monoclonal Ras antibody with the ECL system and by densitometry of corresponding bands using a computing densitometer with Image-Pro plus software.

Preparation of Nuclear Extracts and the Electrophoretic Mobility Shift Assay. A549 cells were cultured in 10-cm culture petri dishes. After reaching confluence, cells were treated with YC-1 or 8-bromo-cGMP for 0~120 min or pretreated with specific inhibitors as indicated followed by YC-1, and then incubated in a humidified incubator at 37°C. The cytosolic and nuclear protein fractions were then separated as described previously (Lin et al., 2001). In brief, cells were washed with ice-cold PBS and then centrifuged. The cell pellet was resuspended in hypotonic buffer (10 mM HEPES, pH 7.9, 10 mM KCl, 0.5 mM DTT, 10 mM aprotinin, 10 mM leupeptin, and 20 mM PMSF) for 15 min on ice, and then vortexed for 10 s. Nuclei were pelleted by centrifugation at 15,000 rpm for 1 min. Supernatants containing cytosolic proteins were collected. A pellet containing nuclei was resuspended in hypertonic buffer (20 mM HEPES, pH 7.6, 25% glycerol, 1.5 mM $MgCl_2$, 4 mM EDTA, 0.05 mM DTT, 10 mM aprotinin, 10 mM leupeptin, and 20 mM PMSF) for 30 min on ice. Supernatants containing nuclear proteins were collected by centrifugation at 15,000 rpm for 2 min, and then stored at −70°C. Nuclear proteins (2.5~5 μg) were incubated with 1 ng of a ^{32}P-labeled NF-κB probe (50,000~75,000 counts/min) in 10 μl of binding buffer [1 μg poly(dI-dC), 15 mM HEPES, pH 7.6, 80 mM NaCl, 1 mM EDTA, 1 mM DTT, and 10% glycerol] at 30°C for 25 min. DNA/nuclear protein complexes were separated from the DNA probe by electrophoresis on 6% polyacrylamide gels; the gels were then vacuum-dried and subjected to autoradiography with an intensifying screen at −80°C. Quantitative data were obtained using a computing densitometer with Image-Pro plus software.

Statistical Analysis. Results are presented as the mean ± S.E.M. from at least three independent experiments. One-way analysis of variance followed by Bonferroni's multiple range test, when appropriate, was used to determine the statistical significance of the difference between means. A p value of less than 0.05 was taken as statistically significant.

Results

Involvement of Ras in YC-1–Induced COX-2 Expression. Our previous results showed that YC-1 induces COX-2 expression in A549 cells (Chang et al., 2002). To investigate the involvement of Ras activation in YC-1–induced COX-2 expression, A549 cells were treated with manumycin A (a Ras inhibitor) (Hara et al., 1993). Pretreatment of cells for 30 min with manumycin A (1~15 μM) attenuated YC-1–induced COX-2 expression in a concentration-dependent manner. Manumycin A (15 μM) completely abolished YC-1–induced COX-2 expression (Fig. 1, A and B). Likewise, long-term pretreatment of A549 cells with manumycin A (1, 10, and 15 μM) for 24 h also inhibited YC-1–induced COX-2 expression in a concentration-dependent manner (data not shown). The YC-1–induced increase in COX activity was also inhibited by 10 μM manumycin A or 0.5 μg of a dominant-negative Ras mutant (RasN17) by 77 ± 3% and 88 ± 2%, respectively (Fig. 1C). We further measured the Ras activity in cells treated with YC-1 or 8-bromo-cGMP, a cell-permeable cGMP analog. As shown in Fig. 2, A and B, treatment of A549 cells with 50 μM YC-1 or 30 μM 8-bromo-cGMP increased the Ras activity in a time-dependent manner. The maximal activation was detected at 5 min after stimulation, and the response contin-

ued until 30 min after stimulation (Fig. 2, A and B). The protein level of Ras was not affected by YC-1 or 8-bromo-cGMP treatment (Fig. 2, A and B). YC-1–induced Ras activity was markedly inhibited by pretreatment of cells for 30 min with 30 μM ODQ (an sGC inhibitor), 3 μM KT-5823 (a PKG inhibitor), and 3 μM manumycin A by 63 ± 5%, 70 ± 5%, and 69 ± 9%, respectively (Fig. 2, C and D). None of these treatments had any effect on Ras expression (Fig. 2C).

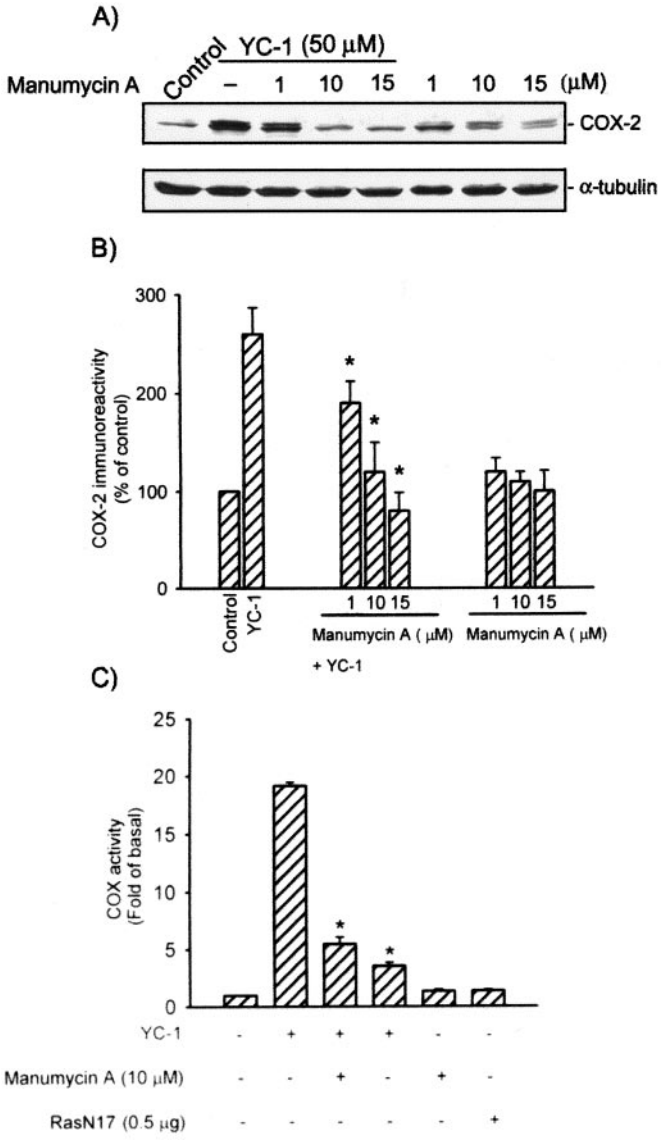

Fig. 1. Involvement of Ras in the YC-1–induced increase of COX-2 expression and COX activity in A549 cells. A, cells were pretreated with various concentrations of manumycin A for 30 min followed by a 12-h YC-1 (50 μM) incubation. Immunodetection with COX-2- or α-tubulin-specific antibodies was performed as described under *Materials and Methods*. Equal loading in each lane was demonstrated by the similar intensities of α-tubulin. B, the extent of COX-2 and α-tubulin protein expression was quantified using a densitometer with Image-Pro Plus software. The relative level was calculated as the ratio of COX-2 to α-tubulin protein levels. Results are expressed as the mean ± S.E.M. (n = 3). *, $p < 0.05$ compared with the YC-1–treated group. C, cells were pretreated with 10 μM manumycin A for 30 min or transfected with 1 μg of a dominant-negative Ras mutant for 24 h before incubation with 50 μM YC-1 for 12 h. The media were then collected, and COX activity was measured by examining PGE_2 formation as described under *Materials and Methods*. Results are expressed as the mean ± S.E.M. of four independent experiments performed in duplicate. *, $p < 0.05$ compared with the YC-1–treated group. RasN17, dominant-negative Ras mutant.

Involvement of PI3K and Akt in YC-1–Induced COX-2 Expression. To determine whether PI3K and its downstream main target, Akt, are involved in the signal transduction pathway leading to COX-2 expression caused by YC-1, cells were treated with a PI3K inhibitor (wortmannin) and an Akt inhibitor (1L-6-hydroxymethyl-chiro-inositol-2-[(*R*)-2-*O*-methyl-3-*O*-octadecylcarbonate]). Pretreatment of cells for 30 min with wortmannin (30 nM) or an Akt inhibitor (10 μM) significantly attenuated the YC-1–induced COX-2 expression by 45 ± 3% and 61 ± 4%, respectively (Fig. 3, A and B). The YC-1–induced increase in COX activity was also inhibited by 30 nM wortmannin or 0.5 μg of a dominant-negative Akt mutant (Akt DN) by 57 ± 2% and 74 ± 2%, respectively (Fig. 3C). Because serine phosphorylation of residue 473 in Akt caused enzymatic activation (Alessi et al., 1996), the antibody specific against phosphorylated Akt (Ser^{473}) was used to examine Akt phosphorylation, an index of kinase activation. Treatment of A549 cells with YC-1 (50 μM) for various time intervals resulted in Akt activation with a maximal response at 10 min after treatment (Fig. 4A). A similar Akt activation pattern was observed in cells treated with 30 μM 8-bromo-cGMP (Fig. 4B). The protein level of Akt was not affected by YC-1 or 8-bromo-cGMP treatment (Fig. 4, A and B). YC-1–induced Akt activation was markedly attenuated by pretreatment of cells for 30 min with ODQ (30 μM), KT-5823 (3 μM), manumycin A (3 μM), or wortmannin (30 nM) by 65 ± 15%, 91 ± 6%, 42 ± 5%, and 83 ± 7%, respectively (Fig. 4, C and D). None of these treatments had any effect on Akt expression (Fig. 4, C and D).

Involvement of Transcription Factor NF-κB in YC-1–Induced COX-2 Expression. To further study the involvement of NF-κB activation in YC-1–induced COX-2 up-regulation, cells were pretreated with the NF-κB inhibitor, pyrrolidine dithiocarbamate (PDTC) (Pan et al., 1995) followed by YC-1. As illustrated in Fig. 5A, pretreatment of cells for 30 min with PDTC (10~50 μM) attenuated YC-1–induced COX-2 expression in a concentration-dependent manner (Fig. 5A). PDTC (50 μM) inhibited YC-1–induced COX-2 expression by 95 ± 2% (Fig. 5B). The YC-1–induced increase in COX activity was also inhibited by 10 μM PDTC by 55 ± 3% (Fig. 5C). To further confirm this result, a dominant negative IκBα mutant (IκBαM) was used. This IκBα mutated form contains serine-to-alanine mutations at residues 32 and 36 and does not undergo signal-induced phosphorylation; thus, it remains bound to NF-κB, ultimately inhibiting NF-κB activation (Chen et al., 1995). Transfection of cells with 1 μg IκBαM inhibited the YC-1–induced increase in COX activity by 72 ± 2% (Fig. 5C). To examine whether YC-1 can induce NF-κB activation, a gel-shift DNA binding assay and pGL2-ELAM-κ B-luciferase assay were conducted. In nuclear extracts of unstimulated cells, a slight intensification of NF-κB–specific DNA-protein complex formation was observed. Stimulation of cells with YC-1 (50 μM) or 8-bromo-cGMP (30 μM) resulted in an increase in NF-κB–specific DNA-protein complex formation in a time-dependent manner, with a maximal effect at 30 min after treatment (Fig. 6, A and B). This gel shift assay detected a specific band produced in the presence of YC-1 or 8-bromo-cGMP, which was outcompeted by an unlabeled 50× competitive probe compared with YC-1 or 8-bromo-cGMP treatment for 30 min (Fig. 6, A and B). In parallel with NF-κB–specific DNA-protein complex formation, when incubating A549 cells with YC-1 (10~50 μM) for

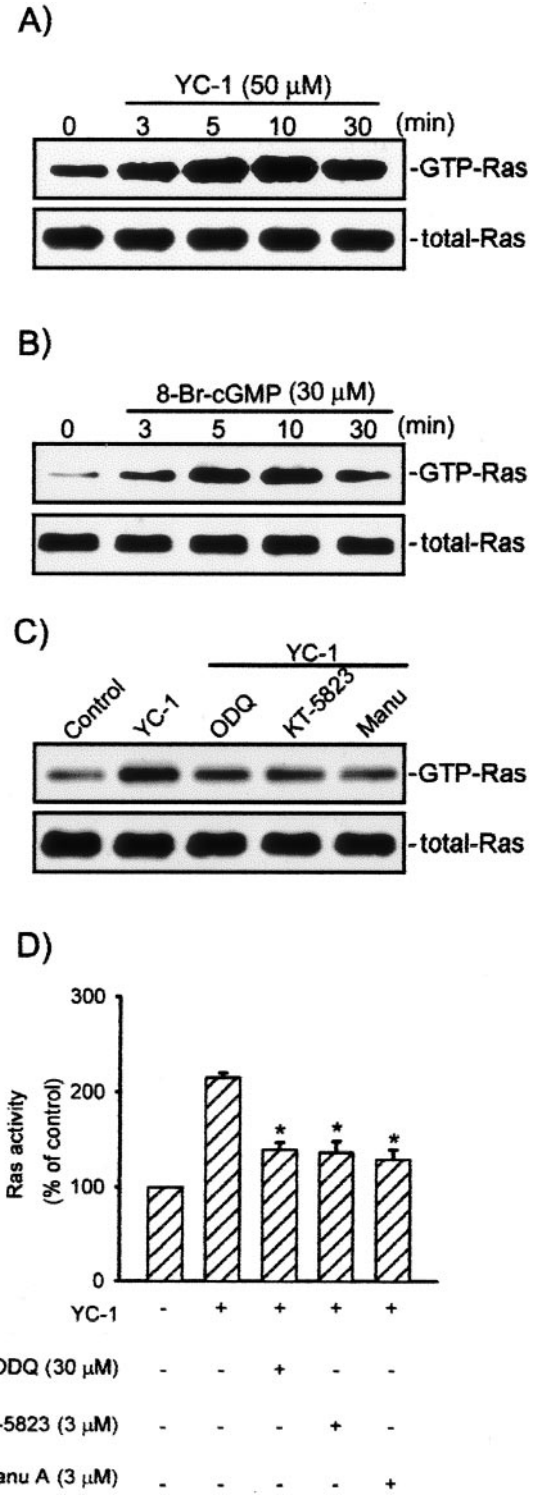

Fig. 2. Effects of ODQ, KT-5823, and manumycin A on the YC-1–induced increase in Ras activity in A549 cells. Cells were treated with 50 μM YC-1 (A) or 30 μM 8-bromo-cGMP (B) for various time intervals, and the Ras activity was measured as described under *Materials and Methods*. C, cells were pretreated with 30 μM ODQ, 3 μM KT-5823, or 3 μM manumycin A for 30 min before incubation with YC-1 (50 μM) for 5 min; then, the Ras activity was measured. Equal amounts in each sample before immunoprecipitation were demonstrated by the similar intensities of total-Ras. D, the extents of GTP-Ras and total-Ras protein from C were quantified using a densitometer with Image-Pro Plus software. The relative level was calculated as the ratio of GTP-Ras to total-Ras protein levels. Results are expressed as the mean ± S.E.M. (n = 3). *, $p < 0.05$ compared with the YC-1–treated group. Manu, manumycin A.

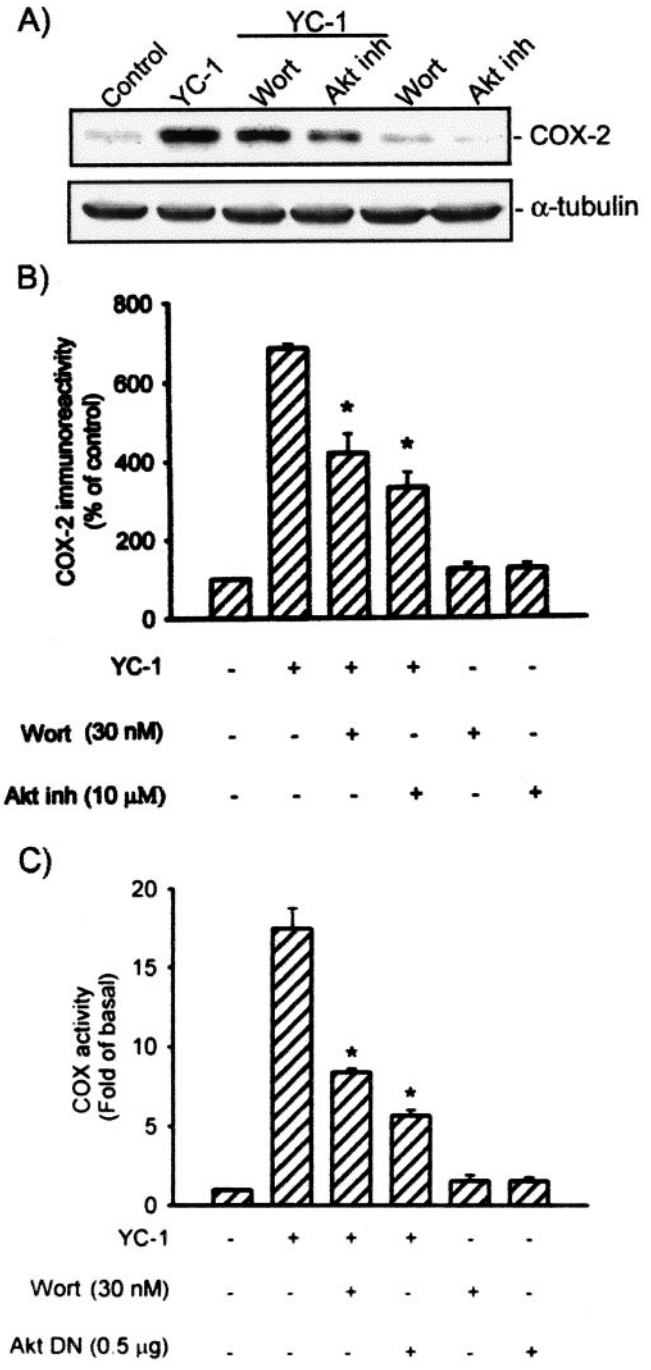

Fig. 3. Involvement of PI3K/Akt in the YC-1–induced increase in COX-2 expression and COX activity in A549 cells. A, cells were pretreated with wortmannin (30 nM) and an Akt inhibitor (10 μM) for 30 min before incubation with YC-1 (50 μM) for 12 h. Cells were then prepared for immunodetection using COX-2- or α-tubulin-specific antibodies as described under *Materials and Methods*. Equal loading in each lane was demonstrated by similar intensities of α-tubulin. In B, the extent of COX-2 and α-tubulin protein expression was quantified using a densitometer with Image-Pro Plus software. The relative level was calculated as the ratio of COX-2 to α-tubulin protein levels. Results are expressed as the mean ± S.E.M (n = 3). *, $p < 0.05$ compared with the YC-1–treated group. C, cells were pretreated with 30 nM wortmannin for 30 min or transfected with 0.5 μg of a dominant negative Akt mutant for 24 h before incubation with 50 μM YC-1 for 12 h. The media were then collected, and the COX activity was measured by examining PGE_2 formation as described under *Materials and Methods*. Results are expressed as the mean ± S.E.M. of four independent experiments performed in duplicate. *, $p < 0.05$ compared with the YC-1–treated group. Akt inh, Akt inhibitor; Wort, wortmannin; Akt DN, dominant-negative Akt mutant.

24 h, a concentration-dependent increase in κB-luciferase activity was observed, with a 235 ± 31% (n = 3) increase when using 25 μM YC-1 (Fig. 6C). Furthermore, we found that pretreatment of cells for 30 min with PDTC (25 μM) inhibited the YC-1–induced increase in κB-luciferase activity by 76 ± 10% (Fig. 6D). Transfection of cells with IκBαM (1 μg) almost completely abolished the YC-1–induced increase in κB-luciferase activity. IκBαM (1 μg) also attenuated the basal κB-luciferase activity by 87 ± 4% (Fig. 6D).

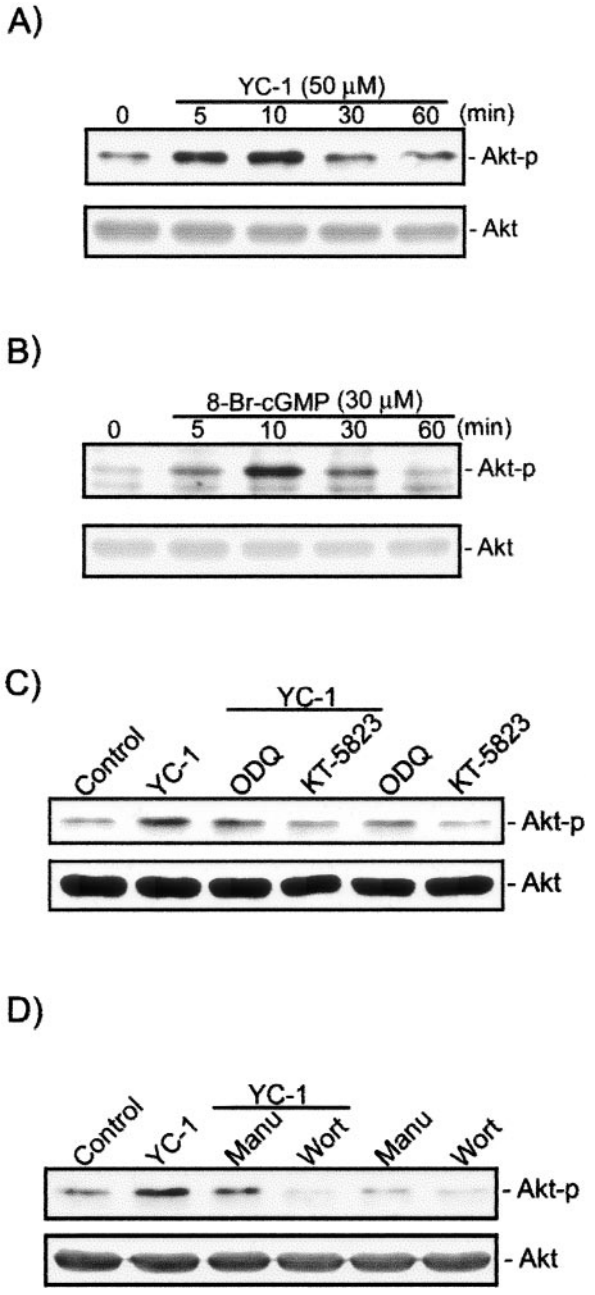

Fig. 4. Effects of ODQ, KT-5823, manumycin A, and wortmannin on YC-1–induced Akt activation in A549 cells. Cells were treated with 50 μM YC-1 (A) or 30 μM 8-bromo-cGMP (B) for various time intervals. Cells were then prepared and subjected to Western blot analysis using antibodies specific for phosphorylated Akt (Ser^{473}) or Akt as described under *Materials and Methods*. Equal loading in each lane is demonstrated by similar intensities of Akt. Data are representative of three independent experiments that gave essentially identical results. C and D, cells were pretreated with 30 μM ODQ, 3 μM KT-5823, 3 μM manumycin A, or 30 nM wortmannin for 30 min before incubation with YC-1 (50 μM) for 10 min. Cells were then prepared and subjected to Western blot analysis as described above. Data are representative of three independent experiments that gave essentially similar results.

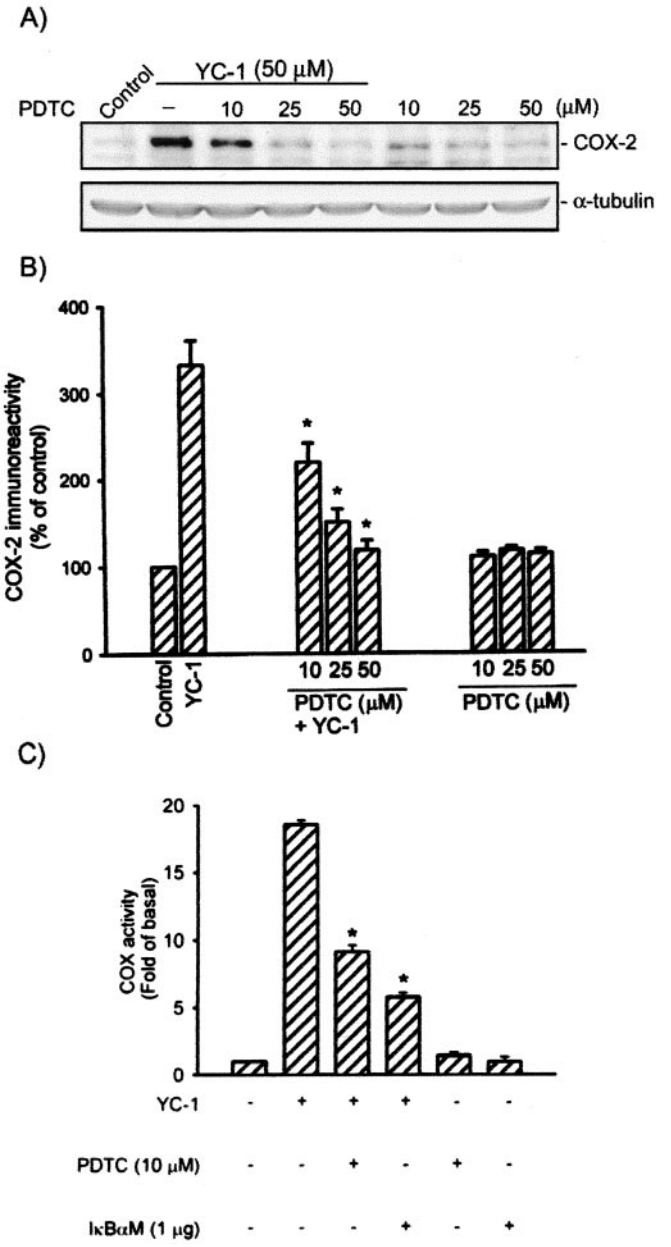

Fig. 5. Involvement of NF-κB in the YC-1–induced increase of COX-2 expression and COX activity in A549 cells. In A, cells were pretreated with PDTC (10~50 μM) for 30 min before incubation with YC-1 (50 μM) for 12 h and then prepared for immunodetection using COX-2- or α-tubulin-specific antibodies as described under *Materials and Methods*. Equal loading in each lane is demonstrated by similar intensities of α-tubulin. B, the extent of COX-2 and α-tubulin protein expression was quantified using a densitometer with Image-Pro Plus software. The relative level was calculated as the ratio of COX-2 to α-tubulin protein levels. Results are expressed as the mean ± S.E.M. (n = 3). *, $p < 0.05$ compared with the YC-1–treated group. C, cells were pretreated with 10 μM PDTC for 30 min or transfected with 1 μg of a dominant negative IκBα mutant for 24 h, before incubation with 50 μM YC-1 for 12 h. The media were then collected, and COX activity was measured by examining PGE_2 formation as described under *Materials and Methods*. Results are expressed as the mean ± S.E.M. of four independent experiments performed in duplicate. *, $p < 0.05$ compared with the YC-1–treated group. IκBαM, dominant-negative IκBα mutant.

YC-1 and 8-bromo-cGMP Induce Increases in IKKα/β Phosphorylation and IKKα/β Activity. We further investigated the upstream molecule involved in the YC-1–induced NF-κB activation signaling pathway. Treatment of A549 cells with 50 μM YC-1 or 30 μM 8-bromo-cGMP induced IKKα/β phosphorylation in a time-dependent manner, beginning at 5 min after treatment and reaching a maximal level at 10~30 min or 10 min after treatment, respectively (Fig. 7, A and B, top). The protein level of IKKα/β was not affected by YC-1 or 8-bromo-cGMP treatment (Fig. 7, A and B, bottom). Furthermore, stimulation of A549 cells with 50 μM YC-1 for 5~60 min also resulted in a marked increase in IKKα/β activity in a time-dependent manner, reaching a maximum after 5~10 min of treatment (Fig. 7C, top). Equal amounts of the immunoprecipitated kinase complex in each kinase assay were confirmed by immunoblotting for the IKKα/β antibody (Fig. 7C, bottom).

PKG, Ras, PI3K, and Akt Mediated YC-1–Induced IKKα/β and NF-κB Activation. To examine whether YC-1–induced increases in IKKα/β phosphorylation, activity and NF-κB activation occur through the PKG/Ras/PI3K signaling pathway, pharmacological inhibitors were applied. Pretreatment of cells for 30 min with wortmannin (30 nM) or an Akt inhibitor (10 μM) markedly abolished YC-1–induced IKKα/β phosphorylation (Fig. 7D, top). None of these inhibitors affected the basal IKKα/β protein level (Fig. 7D, bottom). Pretreatment of cells with ODQ (30 μM), KT-5823 (3 μM), or manumycin A (3 μM) also markedly attenuated the YC-1–induced increase in IKKα/β activity (Fig. 7E). Pretreatment of cells for 30 min with ODQ (30 μM) or KT-5823 (3 μM) almost completely abolished the YC-1–induced increase in κB-luciferase activity (Fig. 8). Pretreatment of cells for 30 min with manumycin A (3 μM), wortmannin (30 nM), or an Akt inhibitor (10 μM) also markedly inhibited the YC-1–induced increase in κB-luciferase activity by 60 $\pm$ 7%, 57 $\pm$ 10%, and 78 $\pm$ 5%, respectively (Fig. 8). Manumycin A (3 μM) and wortmannin (30 nM) attenuated the basal κB-luciferase activity by 33 $\pm$ 12% and 32 $\pm$ 7%, respectively. To further confirm the role of Ras and Akt in YC-1–mediated NF-κB activation, cells were transfected with RasN17 or Akt DN. Transfection of A549 cells with RasN17 or Akt DN inhibited the YC-1–induced increase in κB-luciferase activity by 70 $\pm$ 7% and 87 $\pm$ 13%, respectively. RasN17 (0.5 μg) also inhibited the basal κB-luciferase activity by 25 $\pm$ 11% (Fig. 8).

The Inhibitory Effects of Manumycin A, PDTC, or the Dominant-Negative Mutants of Ras, Akt, and IκBα on YC-1–Induced COX-2 Promoter-Luciferase Activity. We further examined whether the activation of NF-κB is involved in the signal transduction pathway leading to COX-2 expression caused by YC-1. Transient transfections were performed using the human COX-2 promoter-luciferase construct pGS459 (−459/+9). This construct contains both upstream (−447/−438) and downstream (−223/−214) NF-κB sites in the COX-2 promoter. Treatment with 50 μM YC-1 led to a 231 $\pm$ 25% increase in COX-2 promoter-luciferase activity; this effect was inhibited by 10 μM PDTC and IκBαM by

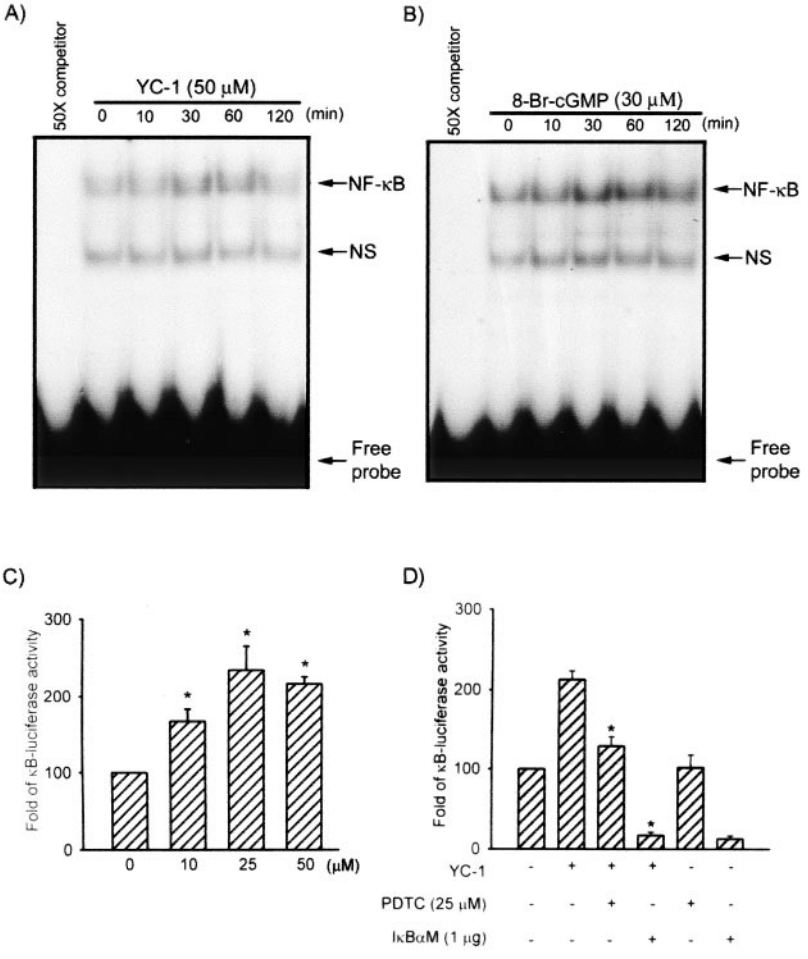

Fig. 6. Kinetics of YC-1- and 8-bromo-cGMP-induced increases in NF-κB-specific DNA-protein complex formation and κB-luciferase activity in A549 cells. Cells were treated with 50 μM YC-1 (A) or 30 μM 8-bromo-cGMP (B) for various time intervals. The nuclear extracts were then prepared, and NF-κB-specific DNA protein complex formation was determined by electrophoretic mobility shift assay as described under *Materials and Methods*. The top band represents NF-κB. Fifty-fold concentrations of unlabeled NF-κB oligonucleotides (50$\times$ competitor) were used for the competition experiment. C, cells were treated with various concentrations of YC-1 (10~50 μM) for 24 h, then harvested for κ B-luciferase assay. D, cells were transiently transfected with 0.5 μg of pGL2-ELAM-Luc and 1 μg of pBK-CMV-Lac Z for 24 h and were either cotransfected with 1 μg of a dominant-negative IκBα mutant or pretreated with 10 μM PDTC for 30 min, before incubation with 25 μM YC-1 for 24 h. Cells were then harvested for the κB-luciferase assay as described under *Materials and Methods*. Results are expressed as the mean $\pm$ S.E.M. (n = 3). *, $p < 0.05$ compared with the YC-1–treated group. NS, nonspecific binding; IκBαM, dominant-negative IκBα mutant.

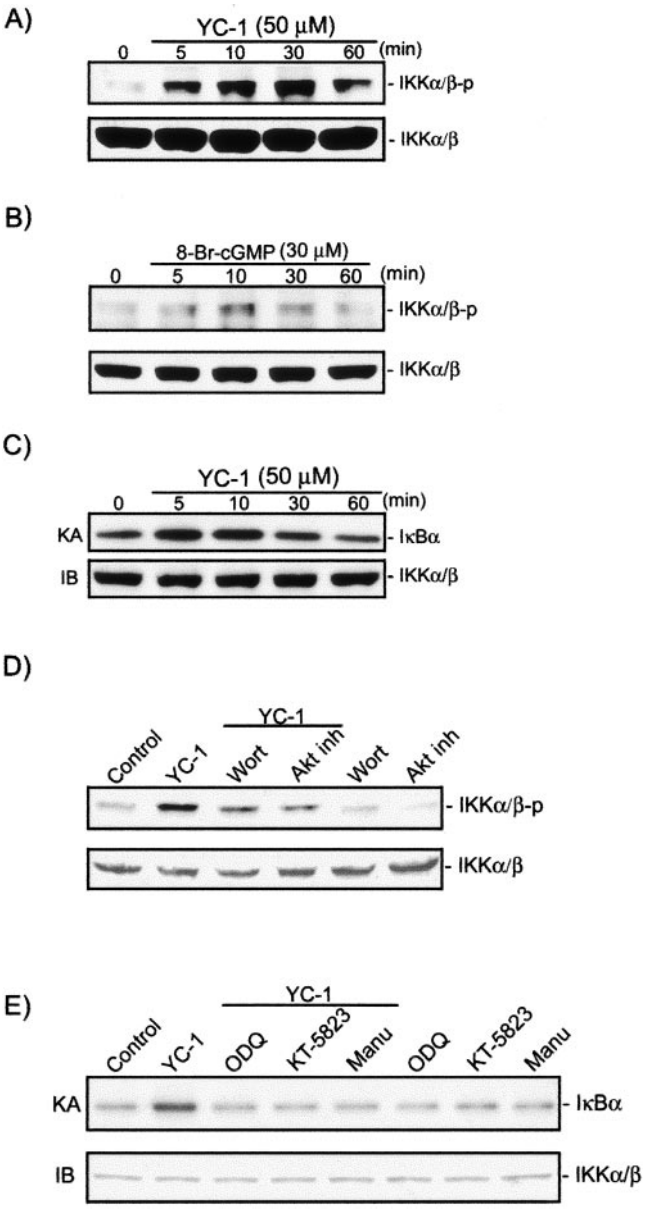

Fig. 7. Effects of ODQ, KT-5823, manumycin A, wortmannin, and an Akt inhibitor on YC-1–induced IKKα/β activation in A549 cells. IKKα/β phosphorylation induced by YC-1 (A) or 8-bromo-cGMP (B) was determined by immunoblotting with a phosphorylated IKKα (Ser180)/IKKβ (Ser181)-specific antibody. Equal loading in each lane is demonstrated by similar intensities of IKKα/β. C, YC-1 time-dependently increased IKKα/β activity. Cells were incubated with 50 μM YC-1 for various time intervals, and cell lysates were then immunoprecipitated with antibodies specific for IKKα or IKKβ. One set of immunoprecipitates was subjected to the kinase assay as described under *Materials and Methods* using the GST-IκBα fusion protein as a substrate (top). The other set of immunoprecipitates was subjected to 10% SDS-PAGE and analyzed by immunoblotting with an anti-IKKα/β antibody (bottom). Equal amounts of the immunoprecipitated kinase complex in each kinase assay were confirmed by immunoblotting for IKKα/β. D, cells were pretreated with 30 nM wortmannin or 10 μM of an Akt inhibitor for 30 min before incubation with 50 μM YC-1 for 10 min. Cell lysates were prepared and subjected to Western blot analysis using antibodies specific for phosphorylated IKKα (Ser180)/IKKβ (Ser181) or IKKα/β. E, cells were pretreated with 30 μM ODQ, 3 μM KT-5823, or 3 μM manumycin A for 30 min before incubation with 50 μM YC-1 for 10 min. Cell lysates were then immunoprecipitated with antibodies specific for IKKα or IKKβ. The kinase assay (top) and immunoblotting analysis (bottom) were performed as described in Fig. 8C. Data are representative of three independent experiments that gave essentially similar results. Wort, wortmannin; Akt inh, Akt inhibitor; Manu, manumycin A; KA, kinase assay; IB, immunoblotting.

62 ± 9% and 78 ± 4%, respectively (Fig. 9). This result further indicates that NF-κB is responsible for mediating the YC-1–induced COX-2 expression in A549 cells. To further confirm the role of Ras and PI3K/Akt in YC-1–induced COX-2 promoter-luciferase activity, manumycin A, RasN17, and Akt DN were used. YC-1–induced COX-2 promoter-luciferase activity was inhibited by 10 μM manumycin A, 0.5 μg of RasN17, and 0.5 μg of Akt DN by 78 ± 4%, 90 ± 5% and, 85 ± 6%, respectively (Fig. 9). Taken together, these results indicated that YC-1 might activate the PKG, Ras, and PI3K/Akt signaling pathways, which in turn activated IKKα/β and NF-κB and finally induced COX-2 expression in A549 cells.

YC-1 Potentiated IL-1β–Induced COX-2 Expression and PGE_2 Release. Our previous study has demonstrated that IL-1β induced COX-2 expression and PGE_2 release in A549 cells (Lin et al., 2000). In A549 cells, we found that YC-1 (50 μM) and IL-1β (0.1 ng/ml) each induced COX-2 expression (Fig. 10A). The combination of YC-1 and IL-1β potentiated the COX-2 expression more than either alone (Fig. 10A). Treatment of A549 cells with IL-1β (0.1 and 1 ng/ml) induced PGE_2 release (Fig. 10B). YC-1 (50 μM) alone did not cause any change in the PGE_2 release (Fig. 10B). However, YC-1 and IL-1β in combination potentiated the increase of PGE_2 release (Fig. 10B).

Discussion

Our previous study showed that YC-1, an activator of sGC, activated protein kinase G through an upstream sGC/cGMP pathway to elicit PKC-α activation, which in turn initiated p44/42 MAPK activation and finally induced COX-2 expression in human pulmonary epithelial cells (A549) (Chang et al., 2002). In the present study, we further demonstrate that Ras, PI3K/Akt, and transcription factor NF-κB might also be involved in the YC-1–induced increase in COX activity and COX-2 expression.

Ras proteins are members of the superfamily of small GTPases claimed to play a key role in signaling pathways

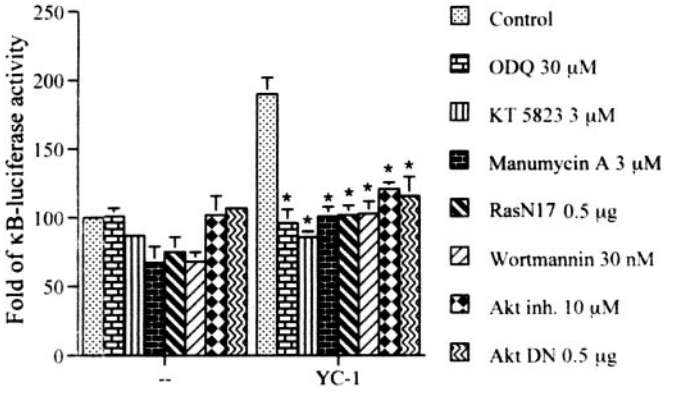

Fig. 8. Effects of various inhibitors or dominant-negative mutants on the YC-1–induced increase in κB-luciferase activity in A549 cells. Cells were transiently transfected with 0.5 μg of pGL2-ELAM-Luc and 1 μg of pBK-CMV-Lac Z for 24 h, were either cotransfected with 0.5 μg of the dominant-negative mutants for Ras or Akt, or pretreated with 30 μM ODQ, 3 μM KT-5823, 3 μM manumycin A, 30 nM wortmannin, or 10 μM Akt inhibitor for 30 min, before incubation with 25 μM YC-1 for 24 h. Cells were then harvested for κB-luciferase assay as described under *Materials and Methods*. Results are expressed as the mean ± S.E.M. (n = 3). *, $p < 0.05$ compared with the YC-1–treated group. RasN17, dominant-negative Ras mutant; Akt inh, Akt inhibitor; Akt DN, dominant-negative Akt mutant.

leading to cell proliferation, differentiation, and transformation (Satoh et al., 1992). Several reports have indicated that Ras might play a critical role in the induction of COX-2 expression in mammary epithelial cell and mast cells (Subbaramaiah et al., 1996; Reddy et al., 2000). In the present study, we show that manumycin A, a Ras farnesyl transferase inhibitor, inhibited the YC-1–induced increase in COX activity, COX-2 expression, and COX-2 promoter-luciferase activity in A549 cells. Furthermore, a Ras dominant-negative mutant (RasN17) also attenuated the YC-1–induced increase in COX activity and COX-2 promoter-luciferase activity. These results suggest that Ras activation might be involved in YC-1–mediated COX-2 expression. Moreover, we demonstrate that treatment of A549 cells with YC-1 or 8-bromo-cGMP resulted in a marked increase in Ras activity. The YC-1–mediated increase in Ras activity was inhibited by ODQ, KT-5823, and manumycin A, suggesting that the YC-1–induced increase in Ras activity occurs downstream of the signal of sGC and PKG.

It has been demonstrated that Ras can directly induce PI3K activation (Rodriguez-Viciana et al., 1994). PI3K activation leads to phosphorylation of phosphatidyl inositides, which then activate the downstream main target, Akt, whose role seems to be important in regulating cellular growth, differentiation, adhesion, and inflammatory reactions (Carpenter and Cantley, 1996; Hirsch et al., 2000). Activation of Akt plays an important role in the Ras-mediated increase in COX-2 mRNA stability and protein expression in Rat intestinal epithelial IEC-6 cells (Sheng et al., 2001). In this study, we demonstrate that the YC-1–induced expression of COX-2 was inhibited by wortmannin (a PI3K inhibitor) and 1L-6-hydroxymethyl-chiro-inositol2-[(*R*)-2-*O*-methyl-3-*O*-octadecylcarbonate] (an Akt inhibitor). The YC-1–induced increase in COX activity was also blocked by wortmannin and a dominant-negative Akt mutant (Akt DN). Furthermore, the YC-1–induced increase in COX-2 promoter-luciferase activity was attenuated by Akt DN. These results indicate that PI3K/Akt activation is involved in signal transduction leading to the expression of COX-2 by YC-1. A previous report indicated that both the NO donor (*S*)-nitroso-*N*-acetylpenicillamine and 8-bromo-cGMP induce Akt activation through the PKG and PI3K pathway in rat PC-12 pheochromo-

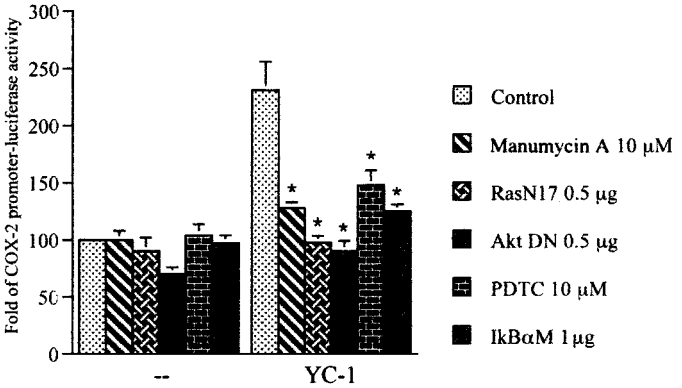

Fig. 9. Effects of various inhibitors or dominant-negative mutants on the YC-1–induced COX-2 promoter-luciferase activity in A549 cells. Cells were transiently transfected with 1 μg of pGS459 (−459/+9) and 1 μg of pBK-CMV-Lac Z for 24 h, and were either cotransfected with the dominant-negative mutants for Ras (RasN17; 0.5 μg), Akt (Akt DN; 0.5 μg) or IκBα (IκBαM; 1 μg), or pretreated with 10 μM manumycin A or 10 μM PDTC for 30 min, before incubation with 25 μM YC-1 for 24 h. Cells were then harvested for the COX-2 promoter-luciferase assay as described under *Materials and Methods*. Results are expressed as the mean ± S.E.M. (n = 3). *, $p < 0.05$ compared with the YC-1–treated group. RasN17, dominant-negative Ras mutant; Akt DN, dominant-negative Akt mutant; IκBαM, dominant-negative IκBα mutant.

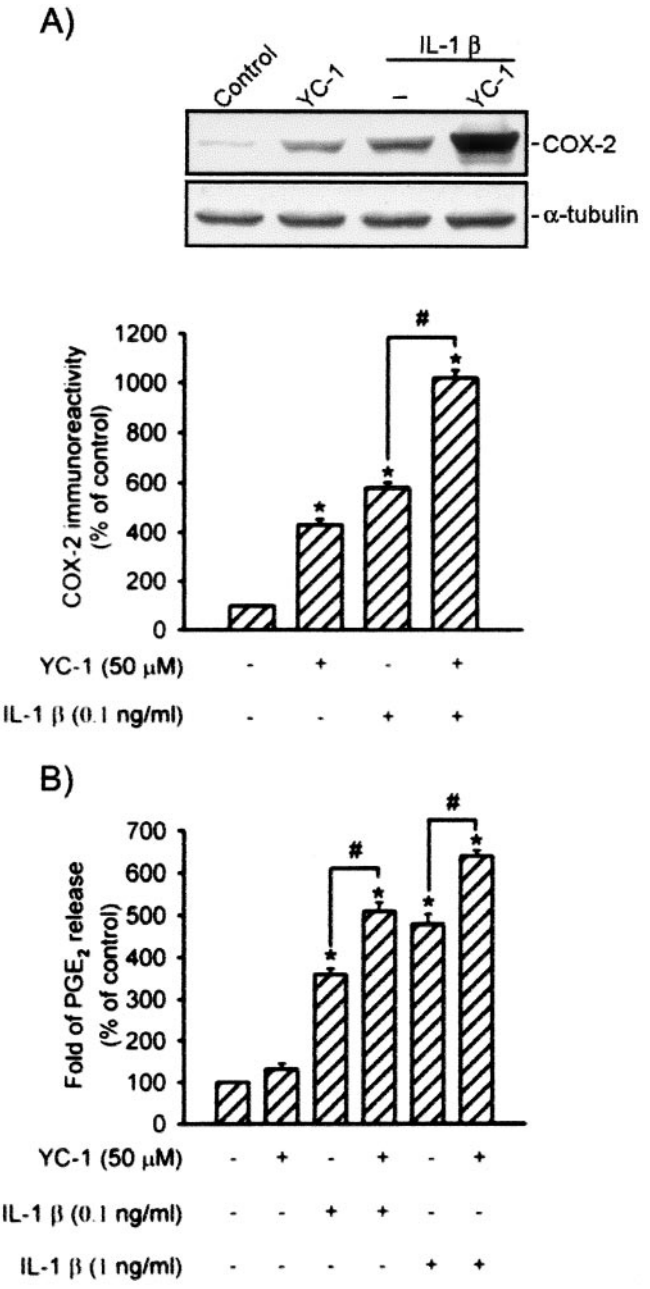

Fig. 10. Effect of YC-1 on IL-1β–induced COX-2 expression and PGE_2 release in A549 cells. A, cells were treated with YC-1 (50 μM), IL-1β (0.1 ng/ml), or a combination of YC-1 (50 μM) and IL-1β (0.1 ng/ml) for 12 h and then prepared for immunodetection using COX-2- or α-tubulin–specific antibodies as described under *Materials and Methods*. Equal loading in each lane is demonstrated by similar intensities of α-tubulin. The extent of COX-2 and α-tubulin protein expression was quantified using a densitometer with Image-Pro plus software. The relative level was calculated as the ratio of COX-2 to α-tubulin protein levels. Results are expressed as the mean ± S.E.M. (n = 3). *, $p < 0.05$ compared with the basal level; #, $p < 0.05$ compared with the IL-1β–treated group. B, cells were treated with YC-1 (50 μM), IL-1β (0.1~1 ng/ml), or a combination of YC-1 (50 μM) and IL-1β (0.1 ~1 ng/ml) for 12 h. The media were then collected, and the release of PGE_2 was measured as described under *Materials and Methods*. Results are expressed as the mean ± S.E.M. of four independent experiments performed in duplicate. *, $p < 0.05$ compared with the basal level; #, $p < 0.05$ compared with the IL-1β–treated group.

cytoma cells (Ha et al., 2003). In the present study, we found that treatment of A549 cells with YC-1 or 8-bromo-cGMP also resulted in marked activation of Akt. YC-1–induced Akt activation was inhibited by an sGC inhibitor (ODQ), a PKG inhibitor (KT-5823), a Ras inhibitor (manumycin A), and a PI3K inhibitor (wortmannin). These results demonstrate for first time that YC-1 activates the sGC/cGMP/PKG pathway to induce Ras/PI3K/Akt activation, which in turn induces COX-2 expression in A549 cells.

The transcription factor NF-κB has been suggested to be important in inflammation, in suppression of apoptosis, and in cell proliferation (Baldwin, 1996; Tak and Firestein, 2001). In addition, NF-κB has been shown to control the induced transcription of the *COX-2* gene (Schmedtje et al., 1997). In this study, we demonstrate that YC-1–mediated COX-2 expression was inhibited by the NF-κB inhibitor PDTC. Moreover, the YC-1–induced increases in COX activity and COX-2 promoter-luciferase activity were attenuated by PDTC and a dominant-negative IκBα mutant (IκBαM). These results indicate that NF-κB was indeed responsible for the YC-1–mediated induction of COX-2 expression in A549 cells. In an inactivated state, NF-κB is normally held in the cytoplasm by the inhibitor protein IκB. Upon stimulation, such as by tumor necrosis factor-α, IκB proteins become phosphorylated by the multisubunit IKK complex, which subsequently targets IκB for ubiquitination, and then are degraded by the 26 S proteasome. Finally, the free NF-κB translocates to the nucleus, where it activates the responsive gene (Chen et al., 2001). In the present study, we found that treatment of A549 cells with YC-1 or 8-bromo-cGMP resulted in increases in IKKα/β phosphorylation, IKKα/β activity, and the formation of NF-κB–specific DNA-protein complex. Using transient transfection with pGL2-ELAM-κB-luciferase as an indicator of NF-κB activity, we also found that YC-1 induced an increase in NF-κB activity and that this effect was blocked by PDTC and IκBαM. A previous report showed that NF-κB activation is mediated via the Ras-dependent signaling pathway, which induces COX-2 transcriptional gene expression in lung epithelial cells (Li et al., 1998). In addition, Romashkova and Makarov (1999) also demonstrated that platelet-derived growth factor may induce NF-κB activation via the Ras/PI3K/Akt/IKK pathway in human skin fibroblasts (Romashkova and Makarov, 1999). In this study, we found that YC-1–induced IKKα/β activation was inhibited by ODQ, KT-5823, manumycin A, wortmannin, and an Akt inhibitor. Furthermore, the YC-1–mediated increase in κB-luciferase activity was inhibited by ODQ, KT-5823, manumycin A, RasN17, wortmannin, an Akt inhibitor, and Akt DN. These results indicate that YC-1 might act through the pathways of PKG, Ras, and PI3K/Akt to induce IKKα/β and NF-κB activation in A549 cells.

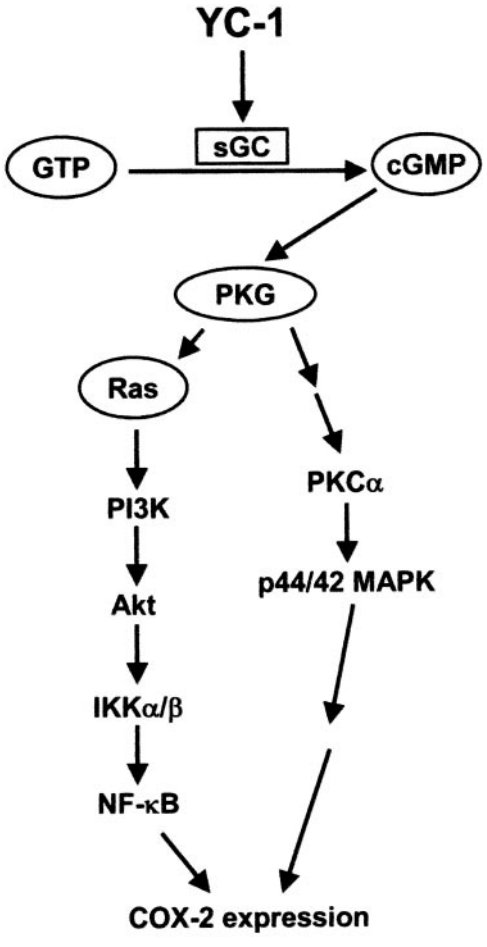

Fig. 11. Schematic diagram illustrating the proposed signaling pathways involved in YC-1–induced COX-2 expression in a human pulmonary epithelial cell line (A549). Treatment of A549 cells with YC-1 caused sGC activation, cGMP accumulation, and PKG activation, which in turn upregulated COX-2 expression through two separate pathways: the Ras/PI3K/Akt cascade to cause IKKα/β and NF-κB activation and the PKC-α -p44/42 MAPK cascade.

PGs, which are formed by the combined action of phospholipase A_2 and COX, play an important role in inflammation and immune response. In our previous study, we found that YC-1 alone did not induce PGE_2 release in A549 cells. When the exogenous arachidonic acid was added, YC-1 markedly increased PGE_2 release. These results suggest that in A549 cells, YC-1 might predominantly cause COX-2 expression but slight or no phospholipase A_2 activation (Chang et al., 2002). In the present study, we found that YC-1 enhanced IL-1β, proinflammatory cytokine-induced COX-2 expression, and PGE_2 release in A549 cells. These results indicate that YC-1–induced COX-2 expression might play a role in enhancing IL-1β-induced PGE_2 release, thus further promoting the immunoregulatory response in A549 cells.

In summary, we demonstrate for the first time that YC-1 might activate the sGC/cGMP/PKG pathway to induce Ras and PI3K/Akt activation, which in turn initiates increases in IKKα/β activity and NF-κB activation, and finally induces COX-2 expression in human lung epithelial cells (A549). The present study, together with our previous report (Chang et al., 2002), delineates, in part, the signaling pathway of YC-1–induced COX-2 expression in human pulmonary epithelial cells (Fig. 11).

Acknowledgments

We are greatly indebted to Prof. Wan-Wan Lin for providing plasmids pGL2-ELAM-Luc and pBK-CMV-Lac Z. We also thank Profs. Che-Ming Teng and C.-C. Chen for providing plasmid Akt DN and pGS459, respectively.

References

Alessi DR, Andjelkovic M, Caudwell B, Cron P, Morrice N, Cohen P, and Hemmings BA (1996) Mechanism of activation of protein kinase B by insulin and IGF-1. *EMBO (Eur Mol Biol Organ) J* **15:**6541–6551.

Baldwin AS Jr (1996) The NF-kappa B and I kappa B proteins: new discoveries and insights. *Annu Rev Immunol* **14:**649–683.
Campbell SL, Khosravi-Far R, Rossman KL, Clark GJ, and Der CJ (1998) Increasing complexity of Ras signaling. *Oncogene* **17:**1395–1413**.**
Carpenter CL and Cantley LC (1996) Phosphoinositide kinases. *Curr Opin Cell Biol* **8:**153–158.
Chang MS, Lee WS, Teng CM, Lee HM, Sheu JR, Hsiao G, and Lin CH (2002) YC-1 increases cyclo-oxygenase-2 expression through protein kinase G- and p44/42 mitogen-activated protein kinase-dependent pathways in A549 cells. *Br J Pharmacol* **136:**558–567.
Chen F, Castranova V, and Shi X (2001) New insights into the role of nuclear factor-kappaB in cell growth regulation. *Am J Pathol* **159:**387–397.
Chen Z, Hagler J, Palombella VJ, Melandri F, Scherer D, Ballard D, and Maniatis T (1995) Signal-induced site-specific phosphorylation targets I kappa B alpha to the ubiquitin-proteasome pathway. *Genes Dev* **9:**1586–1597.
DeWitt DL (1991) Prostaglandin endoperoxide synthase: regulation of enzyme expression. *Biochim Biophys Acta* **1083:**121–134.
Finco TS, Westwick JK, Norris JL, Beg AA, Der CJ, and Baldwin AS Jr (1997) Oncogenic Ha-Ras-induced signaling activates NF-kappaB transcriptional activity, which is required for cellular transformation. *J Biol Chem* **272:**24113–24116.
Franke TF, Kaplan DR, Cantley LC, and Toker A (1997) Direct regulation of the Akt proto-oncogene product by phosphatidylinositol-3,4-bisphosphate. *Science (Wash DC)* **275:**665–668.
Friebe A, Mullershausen F, Smolenski A, Walter U, Schultz G, and Koesling D (1998) YC-1 potentiates nitric oxide- and carbon monoxide-induced cyclic GMP effects in human platelets. *Mol Pharmacol* **54:**962–967.
Hara M, Akasaka K, Akinaga S, Okabe M, Nakano H, Gomez R, Wood D, Uh M, and Tamanoi F (1993) Identification of Ras farnesyltransferase inhibitors by microbial screening. *Proc Natl Acad Sci USA* **90:**2281–2285.
Ha KS, Kim KM, Kwon YG, Bai SK, Nam WD, Yoo YM, Kim PK, Chung HT, Billiar TR, and Kim YM (2003) Nitric oxide prevents 6-hydroxydopamin-induced apoptosis in PC12 cells through cGMP-dependent PI3 kinase/Akt activation. *FASEB J* **17:**1036–1047.
Hirsch E, Katanaev VL, Garlanda C, Azzolino O, Pirola L, Silengo L, Sozzani S, Mantovani A, Altruda F, and Wymann MP (2000) Central role for G protein-coupled phosphoinositide 3-kinase gamma in inflammation. *Science (Wash DC)* **287:**1049–1053.
Hwang TL, Wu CC, and Teng CM (1999) YC-1 potentiates nitric oxide-induced relaxation in guinea-pig trachea. *Br J Pharmacol* **128:**577–584.
Kane LP, Shapiro VS, Stokoe D, and Weiss A (1999) Induction of NF-kappaB by the Akt/PKB kinase. *Curr Biol* **9:**601–604.
Ko FN, Wu CC, Kuo SC, Lee FY, and Teng CM (1994) YC-1, a novel activator of platelet guanylate cyclase. *Blood* **84:**4226–4233.
Li JD, Feng W, Gallup M, Kim JH, Gum J, Kim Y, and Basbaum C (1998) Activation of NF-kappaB via a Src-dependent Ras-MAPK-pp90rsk pathway is required for *Pseudomonas aeruginosa*-induced mucin overproduction in epithelial cells. *Proc Natl Acad Sci USA* **95:**5718–5723.
Lin CH, Kuan IH, Lee HM, Lee WS, Sheu JR, Ho YS, Wang CH, and Kuo HP (2001) Induction of cyclooxygenase-2 protein by lipoteichoic acid from *Staphylococcus aureus* in human pulmonary epithelial cells: involvement of a nuclear factor-κB-dependent pathway. *Br J Pharmacol* **134:**543–552.
Lin CH, Sheu SY, Lee HM, Ho YS, Lee WS, Ko WC, and Sheu JR (2000) Involvement of protein kinase C-γ in IL-1β-induced cyclooxygenase-2 expression in human pulmonary epithelial cells. *Mol Pharmacol* **57:**36–43.
McCormick F (1994) Activators and effectors of ras p21 proteins. *Curr Opin Genet Dev* **4:**71–76.
Mitchell JA, Larkin S, and Williams TJ (1995) Cyclooxygenase-2: regulation and relevance in inflammation. *Biochem Pharmacol* **50:**1535–1542.
Osada M, Tolkacheva T, Li W, Chan TO, Tsichlis PN, Saez R, Kimmelman AC, and Chan AM (1999) Differential roles of Akt, Rac, and Ral in R-Ras-mediated cellular transformation, adhesion and survival. *Mol Cell Biol* **19:**6333–6344.
Pan Z, Kravchenko VV, and Ye RD (1995) Platelet-activating factor stimulates transcription of the heparin-binding epidermal growth factor-like growth factor in monocytes. Correlation with an increased κB binding activity. *J Biol Chem* **270:**7787–7790.
Reddy ST, Wadleigh DJ, and Herschman HR (2000) Transcriptional regulation of the cyclooxygenase-2 gene in activated mast cells. *J Biol Chem* **275:**3107–3113.
Rodriguez-Viciana P, Warne PH, Dhand R, Vanhaesebroeck B, Gout I, Fry MJ, Waterfield MD, and Downward J (1994) Phosphatidylinositol-3-OH kinase as a direct target of Ras. *Nature (Lond)* **370:**527–532.
Rodriguez-Viciana P, Warne PH, Khwaja A, Marte BM, Pappin D, Das P, Waterfield MD, Ridley A, and Downward J (1997) Role of phosphoinositide 3-OH kinase in cell transformation and control of the actin cytoskeleton by Ras. *Cell* **89:**457–467.
Romashkova JA and Makarov SS (1999) NF-kappaB is a target of AKT in anti-apoptotic PDGF signalling. *Nature (Lond)* **401:**86–90.
Satoh T, Nakafuku M, and Kaziro Y (1992) Function of Ras as a molecular switch in signal transduction. *J Biol Chem* **267:**24149–24152.
Schmedtje JF Jr, Ji YS, Liu WL, DuBois RN, and Runge MS (1997) Hypoxia induces cyclooxygenase-2 via the NF-κB p65 transcription factor in human vascular endothelial cells. *J Biol Chem* **272:**601–608.
Sheng H, Shao J, and Dubois RN (2001) K-Ras-mediated increase in cyclooxygenase 2 mRNA stability involves activation of the protein kinase B1. *Cancer Res* **61:**2670–2675.
Smith WL and Marnett LJ (1991) Prostaglandin endoperoxide synthase: structure and catalysis. *Biochim Biophys Acta* **1083:**1–17.
Subbaramaiah K, Telang N, Ramonetti JT, Araki R, DeVito B, Weksler BB, and Dannenberg AJ (1996) Transcription of cyclooxygenase-2 is enhanced in transformed mammary epithelial cells. *Cancer Res* **56:**4424–4429.
Tak PP and Firestein GS (2001) NF-kappaB: a key role in inflammatory diseases. *J Clin Investig* **107:**7–11.
Tulis DA, Bohl Masters KS, Lipke EA, Schiesser RL, Evans AJ, Peyton KJ, Durante W, West JL, and Schafer AI (2002) YC-1–mediated vascular protection through inhibition of smooth muscle cell proliferation and platelet function. *Biochem Biophys Res Commun* **291:**1014–1021.
Vane JR (1994) Pharmacology: towards a better aspirin. *Nature (Lond)* **367:**21519.
Vane JR, Bakhle YS, and Botting RM (1998) Cyclooxygenases 1 and 2. *Annu Rev Pharmacol Toxicol* **38:**97–120.
Williams CS, Mann M, and DuBois RN (1999) The role of cyclooxygenases in inflammation, cancer and development. *Oncogene* **18:**7908–7916.

Address correspondence to: Dr. Chien-Huang, Lin, School of Respiratory Therapy, College of Medicine, Taipei Medical University, 250 Wu-Hsing Street, Taipei 110, Taiwan. E-mail: chlin@tmu.edu.tw